Journal of Engineering Science and Technology Review 17 (4) (2024) 220-225

Research Article

JOURNAL OF
Engineering Science and Technology Review

www.jestr.org

The Mechanism and Effect of Seismic Source Location Using Double Waves in Three-Dimensional Microseismic Monitoring

Zhigang Wang[1,*], Xiaoqing Wang[1], Shunlin Yin[1] and Maochen Ge[2]

[1]*College of Energy Engineering, Xi'an University of Science and Technology, Xi'an, Shaanxi 710054, China*
[2]*Department of Mining Engineering, Missouri University of Science and Technology, Rolla, MO 65409, United States*

Received 13 June 2024; Accepted 24 August 2024

Abstract

Accurate seismic source location has always been the most important purpose of microseismic and seismic monitoring. The location accuracy inside the existing monitoring networks is generally high, whereas the accuracy in the external area and sensor accessories area tends to be low. This scenario contributes to an overall limitation in the effective monitoring area. The seismic source location was performed in this study using P waves and S waves to improve the location accuracy outside the monitoring networks and in the adjacent area and enlarge the high-accuracy control area of the monitoring networks. Moreover, the mechanism of seismic source location was theoretically deduced and clarified utilizing P-S double waves. Then, the location accuracy using the P wave and that using the double waves in three typical three-dimensional monitoring networks was analyzed via numerical simulation. Results demonstrate that, in three-dimensional space, using double waves increase the accuracy control in the radius direction of a monitoring network. With the addition of the S wave, the vertical location error is reduced substantially. The microseismic events in a certain range outside the monitoring networks can also be positioned at high accuracy. The area for precise monitoring has been expanded, and the stability of location results has been improved. This research establishes a basis for the advancement of microseismic monitoring technology, aimed at achieving precise and reliable localization in underground engineering applications.

Keywords: Three-dimensional space, Seismic source location, P waves and S waves, Location mechanism, Location effect

1. Introduction

Since its beginning, microseismic monitoring technology has been investigated by many experts and scholars from different fields (including coal mines, metal mines, hydropower chambers, traffic tunnels, slope stabilization, and shale gas mining) [1–8]. The basic idea involves capturing and analyzing the microseismic signals of rocks generated during rock fracturing to determine their state, fracture time, and position [9]. Seismic source location has become one of the most critical contents in microseismic monitoring systems because it directly influences the analysis of microseismic activity characteristics, calculation of microseismic energy, and predictions of dynamic disasters [10]. Therefore, enhancing the accuracy of seismic source location while expanding the effective monitoring area remains a fundamental challenge in microseismic monitoring research.

Seismic source location mainly aims at picking the first arrival time of microseismic waves via the microseismic signals captured by microseismic sensors and substituting them into the algorithm together with the coordinate of each microseismic sensor to obtain the occurrence position and time of microseismic events through inversion [11]. The P-wave has a higher velocity than other seismic phases, thus, it arrives at the sensor first. The P signal waveform is not easily interfered with when it arrives at the sensor, a characteristic that facilitates precise determination of its first arrival time. Nowadays, scholars primarily perform inversion location by picking the time of the P wave's first arrival. However, the monitored area in three-dimensional spaces, such as underground engineering, is quite complicated, with very limited positions suitable for installing sensors. As a result, many microseismic events occur outside monitoring networks, leading to an inability to pinpoint many disasters accurately. Moreover, engineering sites prefer using a small number of sensors and placing them on the surface or in shallow buried areas related to the project to reduce the installation cost of monitoring networks and minimize installation workload. Sometimes, this approach is the only feasible solution, which considerably aggravates the difficulty in acquiring high-accuracy location results, particularly in the vertical direction.

Some researchers have carried out seismic source location using P-S double waves to enhance the location accuracy of microseismic monitoring networks and improve the location effect [12–14]. The study results obtained through numerical experiments and underground experiments show that the location accuracy is improved to varying degrees. However, microseismic sensors in three-dimensional spaces are not arranged reasonably because of the unclear location mechanism using double waves, thereby triggering large location errors inside and outside monitoring networks, particularly in the vertical direction. Moreover, reducing the installation workload and cost while ensuring the location effect remain challenges that need urgent resolution. Hence, deeply exploring the mechanism of seismic source location via P-S double waves in three-dimensional spaces and realizing the reasonable layout of monitoring networks have great theoretical and practical importance for effectively expanding the area of high-

*E-mail address: zhigangwong@xust.edu.cn
ISSN: 1791-2377
doi:10.25103/jestr.174.24

accuracy monitoring, reducing errors in the vertical direction, and extending the application of microseismic monitoring technology in underground engineering.

On this basis, the seismic source location using the P-S double-wave mechanism in three-dimensional space was expounded through theoretical analysis and numerous numerical calculations. Moreover, the location effect in the three-dimensional space, both outside and inside different monitoring networks was obtained. This research presents great importance for microseismic monitoring to achieve high-accuracy large-area stable locations.

2. State of the art

The accuracy of seismic source locations is affected by various factors, mainly including the spatial coordinate of each microseismic sensor, the propagation speed of microseismic waves, the first arrival time of microseismic signals collected by sensors, the spatial arrangement of sensor arrays, and the seismic source location algorithms [15–18]. Chinese and foreign scholars have extensively explored different influencing factors. For instance, Li et al. [19] investigated how variations in the layout of microseismic monitoring networks, wave velocity, and arrival time errors affect the accuracy of seismic source locations utilizing physical experiments. Seismic source location error is minimized at the center of microseismic monitoring networks, with accuracy progressively decreasing as the distance from the center increases. Additionally, greater errors in wave velocity and arrival time lead to reduced accuracy in seismic source location. The monitoring area can be divided into two subregions by constructing a microseismic hyperbolic governing equation: one dominated by wave velocity errors and the other by arrival time errors. Feng et al. [20] employed a control variable method to investigate the relationship between wave velocity error and seismic source location results within a tunnel. The results demonstrate that the location error increases with the increase in wave velocity error and that these two errors are linearly correlated. On the basis of a microseismic monitoring test in a coal mine, Jia et al. [17] concluded that for the location method that needs to measure the wave velocity in advance, the wave velocity error exhibits a direct impact on the location accuracy; for the location method that does not need to measure the wave velocity, the wave velocity error does not affect the location result. For a fixed monitoring area, the location accuracy improves as the number of sensors increases, provided the sensor count is within a certain range; when it exceeds this value, the location accuracy does not improve further. Li et al. [18] comprehensively analyzed the correlation and convergence of four location algorithms, including classical method, the time difference (TD) method, and the velocity difference (VD) method, which do not require pre-measured velocity, and a new approach called the time method (TM). The TM method, which also does not require pre-measured velocity, is based on a novel objective function involving the joint inversion of seismogenic time and MS source coordinates. They also proposed an adaptive recognition algorithm based on microseismic source location objective functions (ARAOF). The purpose of this algorithm is to select the optimal objective function by evaluating the test data of the monitoring area, the location errors of the four objective functions, and other parameters. The field experiment in an iron mine indicates that the proposed algorithm outperforms the classical method, as well as the TD, VD, and TM methods, in terms of both stability and location accuracy. Li et al. [21] investigated the mechanism by which sensor array layouts affect seismic source location. They noted that the sensor distribution itself does not introduce location errors but can amplify errors in input parameters during the seismic source location process. The study provided optimization principles for the geometric distribution of sensors. These analyses underscore the importance of studying factors such as the layout of microseismic monitoring networks for location accuracy. However, these studies primarily focused on the arrival time and velocity of a single P-wave and their impact on location accuracy for microseismic events occurring within the internal area of monitoring networks. The accuracy of the location around the geometric boundaries formed by monitoring sensors and in the external areas remains unexplored, severely limiting the application of microseismic monitoring technology in underground engineering.

In practical field scenarios, the microseismic signals received by sensors are very complicated. These signals, including not only the P wave but also the S wave and other waves, have been investigated by some scholars. For example, Dong et al. [12] proposed a seismic source location method without measuring the wave velocity in advance (PSAFUVS). They also calculated and fitted seismic source locations by using the arrival times of the P wave and the S wave. The numerical test results show that the accuracy is reasonable and reliable, and this method can determine not only the seismic source location of the unknown velocity system but also the real-time velocity of the P wave and the S wave in each event. Given that the S wave is usually dominant underground, Zhou et al. [13] found that combining the S wave travel time data with the travel time data of at least one P wave from the same event can considerably improve location accuracy. Xu et al. [14] demonstrated that integrating the diffraction stacking of P-wave and S-wave amplitudes for microseismic event moment tensor inversion and localization, validated with two synthetic cases, improves accuracy compared to using only P-wave for source localization. In particular, the antinoise capacity is strong in the vertical direction. Luo et al. [22] proposed a Bayesian location method with variable weights to connect the P-wave and S-wave arrival data for microseismic source location. They also simulated two theoretical events and eight blasting events and concluded that their method effectively reduces pickup errors and improves localization accuracy. Wang Bo [23] concluded from field experiments that utilizing both P-wave and S-wave arrival times for source localization significantly improve accuracy compared to utilizing only P-wave arrival times. This improvement, however, depends on the precise identification of S-wave arrival times. Therefore, the P-S double-wave source location possesses more evident advantages and broader application prospects than the independent use of the P wave. However, the mechanism using double-wave location differs from the single P wave location mechanism. Moreover, research achievements in the three-dimensional spatial mechanism of double-wave location remain lacking.

In the abovementioned studies, the focus has been on the factors influencing seismic source location and the P-S double-wave location effect. While the inclusion of the S-wave improves location accuracy, the fundamental reasons for this improvement—particularly the mechanism

underlying double-wave localization in three-dimensional spaces—remain unclear. Additionally, for common typical three-dimensionally distributed monitoring networks, the location effect using double waves and that using P waves only inside and outside monitoring networks have not been systematically compared and discussed. In the current study, the conventional seismic source location principle and the mechanism for seismic source location utilizing P-S double waves in three-dimensional spaces were theoretically analyzed. Moreover, a numerical simulation program was compiled to compare the location effects with the independent utilization of P waves and the utilization of P-S double waves under three monitoring networks: a monitoring network presenting an approximately two-dimensional distribution, a ring monitoring network where one sensor was laid underground, and a ring monitoring network where three sensors were laid underground. The revealed mechanism of three-dimensional dual-wave seismic source localization effectively explains why the localization results become closer to the actual position with the addition of the S-wave. Dual-wave localization enhances horizontal positioning accuracy and significantly reduces vertical positioning errors, leading to a larger effective monitoring area and more stable, reliable localization outcomes.

The study is structured as follows. In Section 3, the theoretical analysis and the numerical simulation methods and schemes were expounded. In Section 4, the location effects under three differently distributed monitoring networks were analyzed. In Section 5, the entire study was summarized, and pertinent conclusions were drawn.

3. Methodology

3.1 Theoretical analysis

3.1.1 Conventional source location principle

Two sensors (T_1 and T_2) were arranged in three-dimensional space, and a microseismic event was located at point $P_s(x_s, y_s)$. The distance difference Δd from the seismic source to the two sensors was deduced as expressed as follows:

$$\Delta d = V\Delta t \tag{1}$$

where V is the propagation speed of the stress wave, and Δt denotes the time difference when the two sensors (T_1 and T_2) receive the stress wave.

Similar to the two-dimensional conventional seismic source location, the three-dimensional conventional seismic source location adopts the arrival time difference method, for which only the arrival time data of the P wave is utilized. However, in three-dimensional space, the points that meet the conditions are not just a hyperbola but a hyperboloid, as shown in Fig. 1. Two sensors are located at the two focal points of the hyperboloid, and a group of hyperboloids correspond to these two focal points. According to different $V\Delta t$ values in Formula (1), a series of hyperboloids correspond to these two focal points. Two pairs of sensors are often used (one of which is shared by two the pairs). Thus, two sets of hyperboloids are generated. The intersection line corresponding to these hyperboloids is the curve where the computed seismic source positions are located.

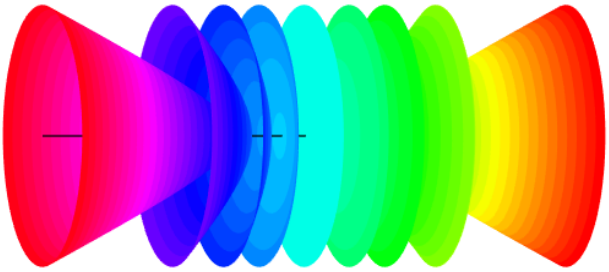

Fig. 1. Hyperboloid field corresponding to the two sensors in the three-dimensional space

In three-dimensional space, two sets of hyperboloid fields corresponding to the two pairs of sensors, T_1/T_2 and T_1/T_3, are shown in Fig. 2. In this case, the number of sensors required for seismic source location is at least four, and the data provided by the three sensors cannot accurately determine the seismic source location. However, Fig. 2 shows that the intersection line of any two hyperboloids is a curve, and the corresponding seismic source location must be on this curve. With the addition of another sensor, the intersection point of the hyperboloid corresponding to one of the existing sensors and this curve is the determined seismic source location.

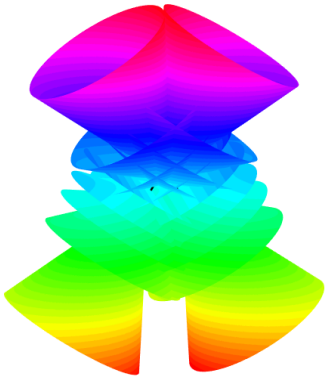

Fig. 2. Hyperboloid field corresponding to the triangularly distributed monitoring networks in the three-dimensional space

In three-dimensional space, the hyperboloid field corresponding to the triangular monitoring network composed of three sensors is shown in Fig. 2. In the monitoring network, the two groups of hyperboloids intersect densely. Near the monitoring network, the intersection density of the two groups of hyperboloids, that is, the density of intersection lines, remains high. However, compared to within the monitoring network, the density of intersection lines has decreased. This finding demonstrates that the accuracy control of seismic source location within the monitoring network is the best. However, the accuracy in the area near the monitoring network is lower compared to that within the network. At farther locations, the density of intersection lines between the two groups of hyperboloids is very small and continuously declines as the distance from the monitoring center continues to increase; that is, the seismic source location accuracy is already very low at farther locations, with significant errors that increase as the distance grows.

3.1.2 Source location mechanism using P-S double waves

In three-dimensional space, seismic source location using P-S double waves is the same as the location mechanism within the plane [24]. The seismic source location algorithm assumes that the stress wave is transmitted linearly from the seismic source to each sensor and then detected and

recognized by each sensor. d is assumed to be the unknown distance between sensor T and the seismic source, C_1 and C_2 stand for the propagation velocities of the P wave and the S wave, respectively, and Δt is the time difference for the S wave and the P wave to arrive at the sensor. Then,

$$d = \frac{C_1 C_2 \Delta t}{C_1 - C_2} \tag{2}$$

If only the P wave velocity C_1 is known, the generally acceptable relationship is $C_2 = 0.6C_1$. In this case, the expression of the unknown number d is simplified into the following form:

$$d = (1.5C_1)\Delta t \tag{3}$$

At this time, the points satisfying Formulas (2) or (3) can form not only a circle but also a spherical surface. Moreover, the sensor is located at the center of the sphere, to which a series of spherical surfaces correspond similarly. The radius of each spherical surface depends on the d value calculated as per Formula (2) or (3).

The three-dimensional space has a pair of sensors. One sensor simultaneously utilizes a P wave and an S wave, whereas the other one uses only a P wave. Their corresponding hyperboloid field and spherical surface field are displayed in Fig. 3. The solved seismic source location is on the intersection line between the corresponding hyperboloid and spherical surface.

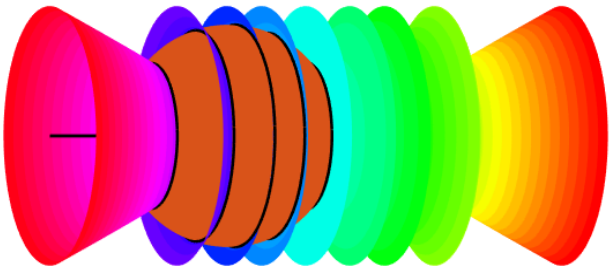

Fig. 3. Hyperboloid field and the spherical surface field corresponding to the two sensors in the three-dimensional space (one sensor adopts P wave and S wave and the other one utilizes only P wave)

The corresponding hyperboloid field and spherical surface field in a triangular microseismic monitoring network are exhibited in Fig. 4. Therein, only one sensor utilizes both waves, whereas the others use only the P wave. The interaction point of the intersection line between any two hyperboloids with the spherical surface is the calculated seismic source location.

The comparison of Fig. 4 and Fig. 2 indicates that the S wave is included, and accuracy control is added in the radial direction of the monitoring network. Hence, the minimum number of sensors required for three-dimensional seismic source location is reduced from 4 to 3. In Fig. 2, the seismic source location is on the intersection line of the corresponding hyperboloids, and at least one additional sensor is needed to determine the specific seismic source location. Fig. 4 shows that the intersection point of the intersection line between any two hyperboloids in the two groups of hyperboloids with the spherical surface is the solved seismic source location.

After the inclusion of the S wave, a spherical surface was added to each sensor accessory. Thus, the monitoring network can accurately locate microseismic events in it and achieve relatively accurate location results for microseismic events near the monitoring network and within a certain range outside it. For microseismic events occurring at great distances, the location error increases as the distance increases. The location accuracy is fundamentally improved by P-S double waves because radial accuracy control is added to the monitoring network.

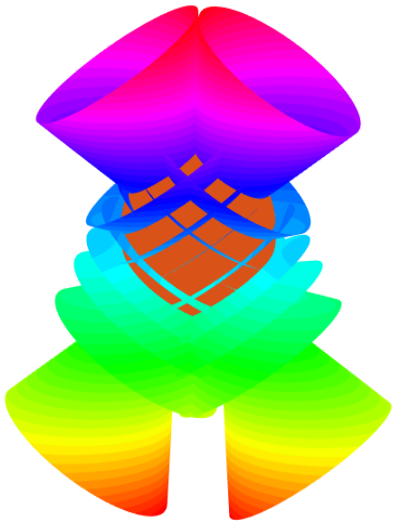

Fig. 4. Hyperboloid field and spherical surface field corresponding to the triangularly distributed monitoring network in the three-dimensional space (one sensor simultaneously utilizes P wave and S wave and the two other ones adopt only P wave)

3.2 Numerical simulation

3.2.1 Simulation method

In this study, a numerical simulation program was developed and executed using MATLAB software. The location results with the independent use of the P wave and the simultaneous use of the P wave and S wave under different monitoring networks were analyzed by this numerical simulation program.

Many calculations were carried out using the numerical simulation method for each point in the monitoring area, i.e.. For each point, numerous computer simulation experiments were performed. In the process of simulation calculation, two errors, namely, wave velocity error and arrival time error, were introduced. In the assumption that P and S waves follow normal distributions $V_p \sim N(\widehat{V}_p, \sigma_{V_p})$ and $V_s \sim N(\widehat{V}_s, \sigma_{V_s})$, respectively, the time errors for the stress wave to arrive at each sensor also follow a normal distribution $\xi \sim N(0, \sigma_t)$. Therefore, the time needed for the P wave to propagate from $P_j(x_j, y_j)$ to sensor T_i is solved as follows:

$$t_{i,j} = \frac{d_{i,j}}{\langle V_p \rangle} + \langle \xi \rangle \tag{4}$$

For the S wave:

$$t_{i,j} = \frac{d_{i,j}}{\langle V_s \rangle} + \langle \xi \rangle \tag{5}$$

where $d_{i,j}$ is the distance between sensor T_i and point P_j, $\langle V_p \rangle$ and $\langle V_s \rangle$ stand for the velocities of the randomly generated P wave and S wave, respectively, and $\langle \xi \rangle$ represents the randomly generated arrival time error.

Then, the randomly generated velocity samples and contaminated arrival time data were used for seismic source location. After various repeated experiments, the seismic source location error for this point is defined as the average distance between the calculated seismic source location $P_j^{'}$ and the actual seismic source location P_j, and is expressed as follows:

$$\sigma(P_j) = \frac{\sum_{k=1}^{N} \sqrt{[(x_j^{'})^k - x_j]^2 + [(y_j^{'})^k - y_j]^2 + [(z_j^{'})^k - z_j]^2}}{N} \quad (6)$$

where N represents the number of repetitions, and $(x_j^{'}, y_j^{'}, z_j^{'})$ denotes the coordinate of point $P_j^{'}$.

In current study, the accuracy of seismic source location was evaluated using the aforementioned method. The number of repetitions (N) was set to 1000, the mean P wave velocity $\widehat{V_p}$ was set to 4,000 m/s, and the standard deviation of P wave velocity σ_{V_p} was set to 400 m/s, i.e., 10% of the mean value. In the assumption that the propagation speed of the S wave is 60% that of the P wave, the propagation S wave velocity $\widehat{V_s}$ is 2,400 m/s, the standard deviation of S wave velocity is 5% of the standard deviation, and the standard deviation of S wave velocity is σ_{V_s} =120 m/s. Moreover, the arrival time error σ_t was set to 0.005 s. The simplex seismic source location algorithm, which is based on the least squares method, was employed to search the optimal seismic source location (L2 norm statistics).

3.2.2 Simulation scheme

To investigate the effectiveness of using the P-S double-wave seismic source location in three-dimensional space, this study analyzed the results of three typical three-dimensional distributed monitoring networks and compared them with results obtained using only the P-wave. The three configurations are as follows: approximately two-dimensional distribution of the monitoring network; one sensor placed underground, with the remaining sensors positioned on the ground in a central circular arrangement; three sensors placed underground, with the other four other sensors located on the ground in a central circular arrangement.

In the monitoring network with an approximate two-dimensional distribution, the number of sensors was set to seven. The entire monitoring network was regularly hexagonal. One sensor was arranged at the center. The network radius was 500 m. Three sensors were laid 10 m beneath the ground surface, whereas the four other ones were placed on the ground surface. The coordinate of each sensor in the monitoring network is displayed in Table 1.

Table 1. Sensor coordinates in the monitoring network with an approximate two-dimensional distribution

Sensor	x/m	y/m	z/m
1	500	0	0
2	250	433	-10
3	-250	433	0
4	-500	0	-10
5	-250	-433	0
6	250	-433	-10
7	0	0	0

One sensor was placed underground, whereas the rest were arranged on the surface in a central circular arrangement. The monitoring network consists of seven sensors configured in a regular pentagon shape, with one sensor located centrally. The network radius was 500 m, with one sensor located 100 m underground and the remaining six sensors placed on the surface. The coordinate of each sensor in the monitoring network is exhibited in Table 2.

Table 2. Sensor coordinates in the monitoring network presenting a ring distribution (with a center, 1 point is 100 m beneath the ground surface)

Sensor	x/m	y/m	z/m
1	500	0	0
2	154.5	475.5	0
3	-404.5	293.9	0
4	-404.5	-293.9	0
5	154.5	-475.5	0
6	0	0	0
7	0	0	-100

Three sensors were placed underground, whereas the four others were located on the surface in a central circular arrangement. Seven sensors were arranged in a configuration resembling an equilateral triangle shape, with one sensor positioned centrally. The distribution radius was 500 m, with three sensors located 100 m underground and the remaining four installed on the surface. The coordinate of each sensor is as seen in Table 3.

Table 3. Sensor coordinates in the monitoring network showing a ring distribution (with a center, 3 points are 100 m beneath the ground surface)

Sensor	x/m	y/m	z/m
1	433	-250	0
2	0	500	0
3	-433	-250	0
4	0	0	0
5	433	-250	-100
6	0	500	-100
7	-433	-250	-100

4. Result Analysis and Discussion

4.1 Location accuracy analysis of the monitoring network presenting an approximately two-dimensional distribution

Fig. 5 shows that the P-wave location accuracy and P-S double-wave location accuracy were high within the monitoring network's range (i.e., within 500 m) regardless of whether the direction was vertical or horizontal. Moreover, the error was approximately 50 m. When only the P wave was used, the location accuracy declined sharply and the error grew rapidly as the distance from the center of the seismic source increased beyond the monitoring network. This outcome is unacceptable in engineering. After the addition of the S wave, the location accuracy remained high within 250 m beyond the monitoring network, the error was approximately 100 m, and the location accuracy steadily

declined as the distance from the monitoring network increased. The horizontal location accuracy was higher than the vertical location accuracy.

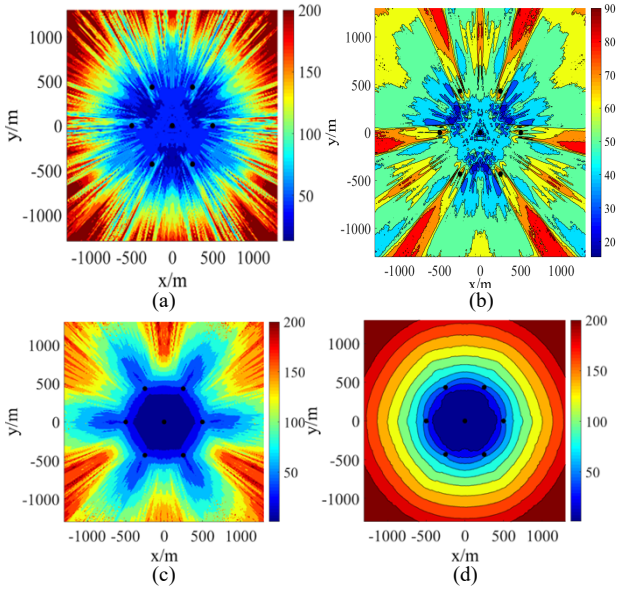

Fig. 5. Location effect of the monitoring network presenting an approximately two-dimensional distribution (-60m level; the black dots represent the projected locations of sensors). (a) Vertical error with independent utilization of P wave. (b) Vertical error with the combined utilization of P wave and S wave. (c) Horizontal error with independent utilization of P wave. (d) Horizontal error with the combined utilization of P wave and S wave

4.2 Location accuracy analysis of the monitoring network presenting a ring distribution with one sensor laid underground

Fig. 6 demonstrates that the location accuracy in the monitoring network remained consistently high, regardless of whether the P wave was used independently or in conjunction with the S wave, and regardless of whether the direction was vertical or horizontal, with the vertical location error being approximately 75 m and horizontal location error being approximately 50 m. When only the P wave was used, the color outside the monitoring network quickly turned from blue to dark red, the location error changed extremely rapidly, and the location effect was rather poor, quickly reaching beyond the localizable range. In the location process using the P wave and the S wave, the location error gradually increased from inside to outside. It even reached 1,000 m outside the monitoring network, and the location error did not exceed 150 m.

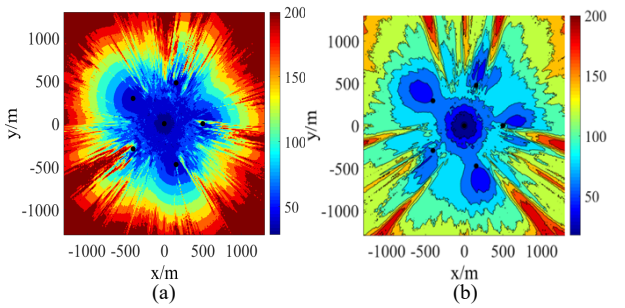

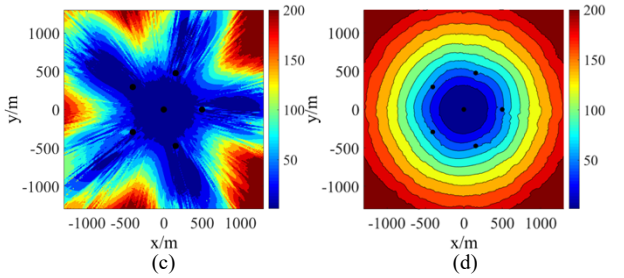

Fig. 6. Location effect (-150m level) in the monitoring network presenting a ring distribution (with a center, 1 point is 100 m beneath the ground surface; the black dots represent the projected locations of sensors). (a) Vertical error with the independent utilization of P wave. (b) Vertical error with the combined utilization of P wave and S wave. (c) Horizontal error with the independent utilization of P wave. (d) Horizontal error with the combined utilization of P wave and S wave

4.3 Location accuracy analysis of the monitoring network presenting a ring distribution with three sensors laid underground

Fig. 7 shows that when only the P wave was used, the location error inside the monitoring network was within 50 m regardless of whether the direction was horizontal or vertical. However, localization was impossible around the sensors, with the color transitioning directly from blue to deep red, and the location error increased to over 200 m. With the combined utilization of the P wave and the S wave, the location error inside the monitoring network did not exceed 30 m. Moreover, the location error gradually grew as the distance from the monitoring network center gradually increased. In addition, the location error was small and changed stably, the reliability was higher, and the location result was closer to the actual location.

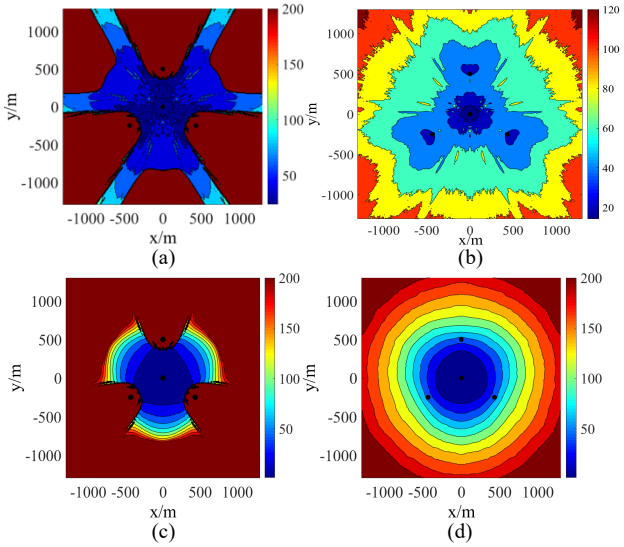

Fig. 7. Location effect (-150m level) in the monitoring network presenting a ring distribution (with a center, 3 points are 100 m beneath the ground surface; the black dots represent the projected locations of sensors). (a) Vertical error with the independent utilization of P wave. (b) Vertical error with the combined utilization of P wave and S wave. (c) Horizontal error with the independent utilization of P wave. (d) Horizontal error with the combined utilization of P wave and S wave

5. Conclusions

The current study aims to extend the effective monitoring area of the microseismic monitoring network in three-dimensional space, especially to improve the vertical monitoring accuracy and the monitoring accuracy near the

monitoring network. This study employed double waves to determine seismic source locations. The location mechanism in three-dimensional space was revealed, and the location results under different sensor layout form were deeply explored through various numerical simulations. Finally, the following key conclusions were drawn:

(1) In three-dimensional space, the mechanism for locating seismic sources utilizing P-S double waves is elucidated. The inclusion of the S wave data is equivalent to adding accuracy control in the radial direction of the monitoring network. Moreover, a spherical surface is added around each sensor.

(2) In the vertical direction, the location accuracy when only the P wave is used is high in most areas within the monitoring network. However, the accuracy of location outside the monitoring network drops sharply to an unacceptable range. After the addition of the S wave, the location accuracy is the highest at the center of the network. The greater the distance from the center is, the lower the location accuracy is. Within a defined range beyond the monitoring network, the location accuracy remains high and declines slowly.

(3) Similar to the situation in the plane, the situation in the horizontal direction shows that the location accuracy is high for the microseismic events within the sensor layout range regardless of whether S wave data are utilized or not. For the microseismic events within a certain external range, high location accuracy can be achieved only after including S wave data. Moreover, the location results are highly reliable.

The mechanism for locating seismic sources utilizing double waves in three-dimensional space is revealed, and the location effects under different sensor layouts are investigated. This study is of particularly great value for microseismic monitoring technology by enabling precise location determination over extensive areas, including great depths, in the three-dimensional geotechnical engineering field. However, the program adopted in this study is a single-wave velocity structure. In practical application fields, the propagation of microseismic waves is quite complicated, and their velocity and path changes are irregular, which may lead to different monitoring effects of microseismic monitoring networks. Therefore, future research should incorporate actual situations in the engineering field and consider varying wave velocity structures to establish more accurate velocity models. This will enhance the precision and stability of microseismic event localization over larger areas.

Acknowledgements

This work was supported by the National Natural Science Foundation of China under Grant No. 52204155.

References

[1] C. Zhang *et al.*, "Prediction of rockbursts in a typical island working face of a coal mine through microseismic monitoring technology," *Tunn. Undergr. Sp. Tech.*, vol. 113, Jul. 2021, Art. no. 103972, doi: 10.1016/j.tust.2021.103972.

[2] G. Y. Si *et al.*, "Seismic monitoring and analysis of excessive gas emissions in heterogeneous coal seams," *Int. J. Coal Geol.*, vol. 149, no. 1, pp. 41-54, Sept. 2015, doi: 10.1016/j.coal.2015.06.016.

[3] D. Zhang. *et al.*, "An effective denoising method based on cumulative distribution function thresholding and its application in the microseismic signal of a metal mine with high sampling rate (6 kHz)," *Front. Earth Sc-switz.*, vol. 10, Jul. 2022, Art. no. 933284, doi: 10.3389/feart.2022.933284.

[4] P. W. Xiao, T. B. Li, N. W. Xu, Z. Zhou, and X. H. Liu, "Microseismic monitoring and deformation early warning of the underground caverns of Lianghekou hydropower station, Southwest China," *Arab. J. Geosci.*, vol. 12, no. 16, Aug. 2019, doi: 10.1007/s12517-019-4683-7.

[5] X. Zhou, B. Li, C. M. Yang, W. M. Zhong, Q. F. Ding, and H. Y. Mao, "Stability analysis of surrounding rock in multi-discontinuous hydraulic tunnel based on microseismic monitoring," *Appl. Sci.*, vol. 12, no. 1, Jan. 2022, doi: 10.3390/app12010149.

[6] X. Z. Liv, C. A. Tang, L. C. Li, P. F. Lv, and R Sun, "Microseismic monitoring and stability analysis of the right bank slope at Dagangshan hydropower station after the initial impoundment," *Int. J. Rock Mech. Min.*, vol. 108, pp. 128-141, Aug. 2018, doi: 10.1016/j.ijrmms.2018.06.012.

[7] X. Luo, M. Salvoni, P. Dight, and J. Duan, "Microseismic events for slope stability analysis - a case study at an open pit mine," *J. S. Afr. I. Min. Metall.*, vol. 118, no. 3, pp. 205-210, Mar. 2018, doi: 10.17159/2411-9717/2018/v118n3a2.

[8] A. K. Hart, "3D seismic attribute-assisted analysis of microseismic events in the Marcellus Shale," M. S. thesis, Dept. Geol. Geogr., West Virginia Univ., USA, 2015.

[9] J. X. Hou *et al.*, "Numerical simulation of rock moving process of combined open-pit and underground mining based on microseismic monitoring and rock mass damage model," (in Chinese), *Chinese J. Rock Mech. Eng.*, vol. 43, no. S1, pp. 3243-3256, May 2024, doi: 10.13722/j.cnki.jrme.2023.0151.

[10] H. S. Zha *et al.*, "Microseismic monitoring on limestone water inrush at coal seam floor for group A coal layer of Pan'er Coal Mine," (in Chinese), *J. China Coal Soc.*, vol. 47, no. 8, pp. 3001-3014, Aug. 2022, doi: 10.13225/j.cnki.jccs.WX22.1075.

[11] A. Y. Cao *et al.*, "High-precision phase picking and automatic source locating method for seismicity in mines based on deep transfer learning," (in Chinese), *J. China Coal Soc.*, vol. 48, no. 12, pp. 4393-4405, Apr. 2023, doi: 10.13225/j.cnki.jccs.2023.0095.

[12] L. J. Dong, and X. B, Li, "A microseismic/acoustic emission source location method using arrival times of PS waves for unknown velocity system," *Int. J. Distrib. Sens. N.*, vol. 9, no. 10, Oct. 2013, doi.: 10.1155/2013/307489.

[13] H. Zhou, W. Zhang, and J. Zhang, "Downhole microseismic monitoring for low signal-to-noise ratio events," *J. Geophys. Eng.*, vol. 13, no. 5, pp. 805-816, Oct.2016, doi: 10.1088/1742-2132/13/5/805.

[14] J. C. Xu, W. Zhang, X. Liang, J. J. Rong, and J. L. Li, "Joint microseismic moment-tensor inversion and location using P- and S-wave diffraction stacking," *Geophysics*, vol. 86, no. 6, pp. KS137-KS150, Nov. 2021, doi: 10.1190/GEO2021-0104.1.

[15] J. Z. Zhang, H. Liu, Z. H. Zou, and Z. L. Huang, "Velocity modeling and inversion techniques for locating microseismic events in unconventional reservoirs," *J. Earth Sci.-China*, vol. 26, no. 4, pp. 495-501, Aug. 2015, doi: 10.1007/s12583-015-0565-4.

[16] P. Wang, X. Chang, and X. Y. Zhou, "Estimation of the relative arrival time of microseismic events based on phase-only correlation," *Energies*, vol. 11, no. 10, Oct. 2018, doi: 10.3390/en11102527.

[17] B. X. Jia, L. L. Zhou, Y. S. Pan, and H. Chen, "Artificial seismic source field research on the impact of the number and layout of stations on the microseismic location error of mines," *Adv. Civ. Eng.*, vol. 2019, no. 1, Jan. 2019, Art. no. 1487486, doi: 10.1155/2019/1487486.

[18] T. Li, B. R. Chen, X. H. Zhu, X. Wang, and M. X. Xie, "Research on the objective function of microseismic source location andits adaptive recognition algorithm," *Chinese J. Rock Mech. Eng.*, vol. 40, no. S2, pp. 3137-3146, Nov. 2021, doi: 10.13722/j.cnki.jrme.2021.0677.

[19] N. Li, "Research on mechanisms of key factors and reliability for microseismic source location," (in Chinese), Ph.D. dissertation, Sch. Safety Eng., China Univ. Min. Technol., Xuzhou, Jiangsu, 2014.

[20] G. L. Feng, X. T. Feng, B. R. Chen, Y. X. Xiao, and Q. Jiang, "Sectional velocity model for microseismic source location in tunnels," *Tunn. Undergr. Sp. Tech.*, vol. 45, pp. 73-83, Jan. 2015, doi: 10.1016/j.tust.2014.09.007.

[21] N. Li, M. C. Ge, E. Y. Wang, and S. H. Zhang, "The influence mechanism and optimization of the sensor network on the MS/AE source location," *Shock Vib.*, vol. 2020, no. 1, Sep. 2020, Art. no. 2651214, doi: 10.1155/2020/2651214.

[22] Z. H. Luo, X. Y. Shang, Y. Wang, X. B. Li, L. H. Liu, and Y. Tai, "P- and S-wave arrival time combined Bayesian location method fora microseismic event," *J. Cent. South Univ.*, vol. 30, no. 11, pp. 3808-3820, Dec. 2023, doi: 10.1007/s11771-023-5459-5.

[23] B. Wang, "Study on the influence of S-wave arrival time on thelocation of microseismic source and how to deal with it," (in Chinese), M. S. thesis, Coll. Geophys. Petrol. Resour., Yangtze Univ., Wuhan, Hubei, 2019.

[24] Z. G. Wang, J. Li, and B. Li, "Source location mechanism of microseismic monitoring using P-S waves and its effect analysis," *Dyna.*, vol. 97, no. 1, pp. 39-45, Jan. 2022, doi: 10.6036/10370.